Pergamon

Int. J. Heat Mass Transfer. Vol. 38, No. 2, pp. 339–350, 1995

0017-9310/95 $9.50+0.00

0017-9310(94)00129-4

Mass transfer limited drying of porous media containing an immobile binary liquid mixture

CLIFFORD K. HO† and KENT S. UDELL‡

Department of Mechanical Engineering, University of California, Berkeley, CA 94720, U.S.A.

(*Received* 5 *April* 1993 *and in revised form* 30 *March* 1994)

Abstract—A theory was developed to predict transient effluent concentrations, liquid concentrations, and the position of the evaporation front during external (mass transfer limited) drying of a porous material containing an immobile binary liquid mixture. One-dimensional drying experiments were performed with different binary mixtures to assess the validity of the model. Theoretical and experimental findings showed that the evaporation during mass transfer limited drying was non-selective in terms of component volatility; the mass fractions of the compounds in the effluent gas remained near the mass ratio of the emplaced liquid mixture. The effluent concentrations and the velocity of the evaporation front were shown to be proportional to $t^{-1/2}$. A growing zone of variable liquid concentrations was shown to exist near the penetrating evaporation front.

INTRODUCTION

Drying of porous materials is an important process in many food, manufacturing, and processing industries. In most applications, drying occurs in response to the flow of heated air over a material which is wetted with a single-component liquid—typically water. Numerous investigators have studied this particular subject to determine drying rates, moisture content, and temperature distributions within a porous material [1–13]. An area which has received far less attention is that of multicomponent drying. In this case the material being dried is wetted with a mixture rather than a single component. Applications include the drying of pharmaceutical products, lacquers, photographic films, and foodstuffs [14].

Another recent and important process which concerns multicomponent drying of porous media is the remediation of hydrocarbon-contaminated soils by a method called soil vapor extraction or soil venting. In this application airflow is usually induced through a contaminated region of soil. Vacuum pumps are connected to wells which are placed in the contaminated soil [15]. The liquid contaminants are then vaporized and removed from the soil in the extracted gas phase. Ideally, the path of airflow would be through the region of contamination. However, due to heterogeneities in the subsurface, channeling often causes the air to bypass regions of contamination as shown in Fig. 1 [16]. This condition is commonly referred to as diffusion-controlled or mass transfer limited venting since the rate of hydrocarbon recovery is limited by vapor phase diffusion from the stagnant regions of contamination to the convective region of airflow [16–18]. Due to the low initial contaminant liquid saturations, this situation is analogous to the decreasing-rate period of drying in which an evaporation front penetrates into the regions of minimal airflow. However, in previous studies on this subject the material being dried was wetted with only a single-component liquid [19–25].

Although many investigators have studied the mechanisms of drying during soil venting, nearly all of the research has been done assuming a through-flow condition [26–28]. A few have investigated the diffusion-controlled process for a single component [15, 29], but a quantitative description of multicomponent drying during the decreasing-rate period has not been established. Thurner and Schlünder [30] have investigated drying of porous materials wetted with a binary mixture during the constant-rate period assuming a constant liquid velocity due to capillary suction, but they do not consider the receding evaporation front which is prominent during diffusion-controlled venting of residually contaminated soils.

The purpose of this study is to investigate the diffusion-controlled venting process as it applies to the drying of porous media containing an immobile binary liquid mixture. A theoretical model is developed to predict the effluent concentration of each component, the position of the evaporation front, and the composition of the liquid mixture during the drying process. Experiments are performed with different binary mixtures in a one-dimensional experiment to determine these variables. Finally, a comparison between the results of the theory and experiments is made, and conclusions are drawn based on these findings.

†Currently at Sandia National Laboratories, P.O. Box 5800, Albuquerque, NM 87185-1324, U.S.A.

‡Author to whom correspondence should be addressed.

NOMENCLATURE

A, B	components in the binary mixture
A_c	cross-sectional area of the porous material
c_t	total molar concentration of the liquid [mol (m^3 liquid)$^{-1}$]
C_{ave}	concentration in the effluent gas
$C^{(1)}$	concentration of the gas in the dry region [kg (m^3 gas)$^{-1}$]
$C_g^{(2)}$	concentration of the gas in the wet region [kg (m^3 gas)$^{-1}$]
$C_l^{(2)}$	concentration of the liquid in the wet region [kg (m^3 liquid)$^{-1}$]
C_{sat}	concentration of the gas at the evaporation front [kg (m^3 gas)$^{-1}$]
$D^{(1)}$	effective gas diffusion coefficient in the dry region [m^2 s^{-1}]
$D^{(2)}$	effective overall gas–liquid diffusion coefficient in the wet region [m^2 s^{-1}]
$D_g^{(2)}$	effective gas diffusion coefficient in the wet region [m^2 s^{-1}]
$D_l^{(2)}$	effective liquid diffusion coefficient in the wet region [m^2 s^{-1}]
$\mathscr{D}^{(1)}$	$D^{(1)}/(\phi_t+\beta_i)$ [m^2 s^{-1}]
$\mathscr{D}^{(2)}$	$D^{(2)}/(S_l\phi_t)$ [m^2 s^{-1}]
erf (x)	error function, $(2/\sqrt{\pi})\int_0^x e^{-\xi^2}\,d\xi$
erfc	$1-\text{erf}\,(x)$
M	molecular weight [kg kmol^{-1}]
p	partial pressure [Pa]
Q	volumetric air flow rate [m^3 s^{-1}]
R	universal gas constant [8314.4 N m kmol^{-1} K^{-1}]
S_l	liquid saturation [m^3 liquid (m^3 pore space)$^{-1}$]
t	time [s]
T	temperature [K]
x	liquid mole fraction [mol mol^{-1}]
z	distance from surface of porous media [m].

Greek symbols

α	local equilibrium conversion factor [m^3 liquid (m^3 gas)$^{-1}$]
β	slope of linear adsorption isotherm {kg ads (m^3 total)$^{-1}$ [kg (m^3 gas)]$^{-1}$}
δ	position of penetrating evaporation front [m]
γ	activity coefficient [mol mol^{-1}]
κ_1, κ_2	numerical constants [kg m^{-3}]
ϕ_a	air-filled porosity [m^3 gas (m^3 total)$^{-1}$]
ϕ_t	total porosity [m^3 pore (m^3 total)$^{-1}$].

Subscripts

amb	ambient conditions
ave	average
f	final
g	gas phase
i	denotes either component A or component B
l	liquid phase.

Superscripts

(1)	dry region
(2)	wet region
0	initial or pure component.

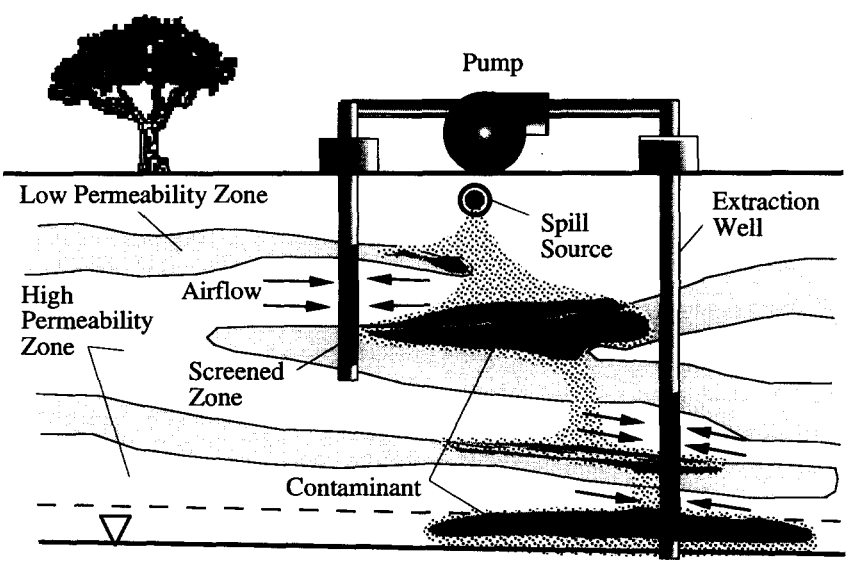

Fig. 1. Basic soil venting system in a heterogeneous, hydrocarbon-contaminated subsurface.

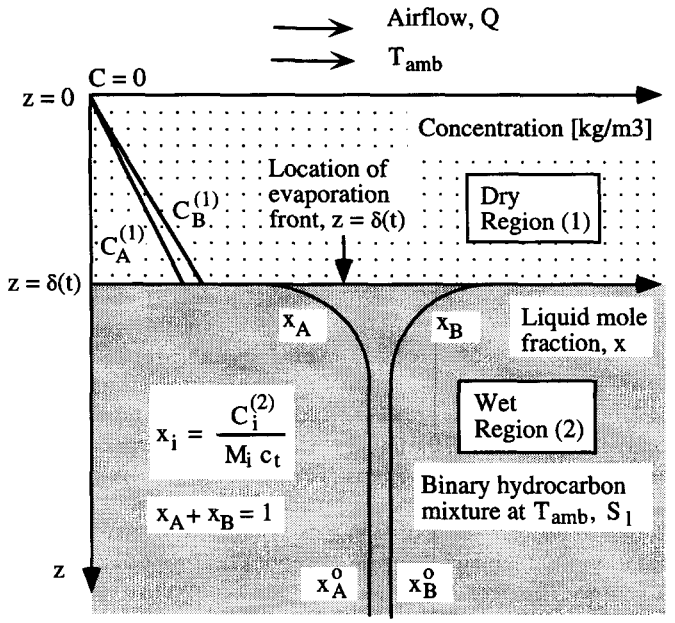

Fig. 2. Model for one-dimensional, external convective drying of a porous medium containing an immobile binary liquid mixture during the period of the penetrating evaporation front.

THEORETICAL WORK

The physical system being considered is the porous half-space partially wetted with an immobile binary liquid mixture as shown in Fig. 2. For $t > 0$ ambient air flows over the material, and evaporation of the liquid causes an evaporation front to penetrate into the porous material to a location $z = \delta(t)$. We assume that both components, A and B, are completely vaporized at this penetrating front (i.e. $\delta_A = \delta_B = \delta$), and this condition will be shown to exist in the experiments. Two regions can then be considered in the analysis: (1) a dry region containing only gas phase components which extends from the surface ($z = 0$) to the evaporation front [$z = \delta(t)$], and (2) a wet region consisting of both liquid and gas phase components which extends from the evaporation front to $z = \infty$. Initially, the liquid mixture occupies the entire half-space and is assumed to have a uniform composition:

$$C_{l,i}^{(2)}(z, t = 0) = C_{l,i}^{0} \tag{1}$$

where C is the concentration, the subscript l denotes the liquid phase in the wet region, the subscript i represents either component A or component B, the superscript (2) denotes the wet region, and $C_{l,i}^{0}$ refers to the initial liquid concentration of component i. The liquid concentration is defined as follows:

$$C_{l,i}^{(2)}(z, t) = x_i(z, t)\, M_i c_t \tag{2}$$

where x_i is the liquid mole fraction of component i, M_i is the molecular weight of component i, and c_t is the molar concentration of the liquid. The molar concentration, c_t, is assumed to be constant at the initial molar concentration of the mixture.

In this model, the liquid saturation, S_l, is assumed constant in the wet region based on experiments by Cunningham and Kelly [31]. They showed that, when liquid saturations dropped to values near 0.1 during external drying, the saturation was nearly constant in the wet region. Isothermal conditions are also assumed to exist in the half-space based on the observations of Szentgyörgyi [9]. In this study uniform temperatures were observed in the wet region during the period of the penetrating evaporation front, but the temperatures gradually increased because of the heated external flow. In this study, both the external airflow temperature and the initial liquid temperature are at ambient conditions. Localized depressed temperatures caused by evaporation are slight and are not expected to alter the temperatures elsewhere since evaporation rates are slow compared to the heat transfer from surrounding regions during the period of the penetrating evaporation front. Therefore, isothermal conditions are assumed to exist with the temperature equal to the ambient temperature, T_{amb}. Fixed boundary conditions corresponding to the situation shown in Fig. 2 can be stated as follows:

$$C_i^{(1)}(z = 0, t) = 0 \tag{3}$$

$$C_{l,i}^{(2)}(z \to \infty, t) = C_{l,i}^{0} \tag{4}$$

where the superscript (1) denotes the dry region and $C_i^{(1)}$ is the gas phase concentration of component i in the dry region. The first condition implies that sufficient airflow at the surface ($z = 0$) causes the gas phase concentration to be zero there. The second condition implies that the resistance to mass transfer is large in the wet region. Consequently, at a distance sufficiently far from the surface the composition of the liquid remains unchanged from its initial composition. Thermodynamic equilibrium and mass continuity at

the moving interface of the dry and wet zones [$z = \delta(t)$] can be used to obtain two more boundary conditions at the evaporation front:

$$C_i^{(1)}(z = \delta(t), t) = \alpha_i C_{l,i}^{(2)}(z = \delta(t), t) = C_{sat,i} \quad (5)$$

$$D_i^{(1)} \left.\frac{\partial C_i^{(1)}}{\partial z}\right|_{z=\delta} - D_i^{(2)} \left.\frac{\partial C_{l,i}^{(2)}}{\partial z}\right|_{z=\delta} = \frac{S_l \phi_t C_{sat,i}}{\alpha_i} \frac{d\delta(t)}{dt} \quad (6)$$

where

$$\alpha_i = \frac{\gamma_{il} p_i^0}{c_t RT} \quad (7)$$

γ_{il} is the activity coefficient of component i in the liquid mixture, p_i^0 is the vapor pressure of component i, R is the gas constant, and T is the absolute temperature. Equation (5) states that the gas concentration of each component at the evaporation front remains at a constant value, C_{sat}, for $t > 0$. This condition was observed experimentally by Heimann *et al.* [32] during the constant-rate period of drying. Local equilibrium between the gas and liquid phases is assumed to exist in the wet region so that the gas and liquid concentrations can be related by the local equilibrium factor, α_i. This factor was derived from the ideal gas law and the definition of the partial pressure of a component in a mixture: $p_i = x_i \gamma_{il} p_i^0$.

Equation (6) enforces conservation of mass across the evaporation front. The term on the right-hand side represents an amount of mass which is liberated from the liquid phase as the front moves a distance $d\delta$. The terms on the left represent diffusion on both sides of the front where $D_i^{(1)}$ is the effective gas diffusion coefficient of component i in the dry region and $D_i^{(2)}$ is the effective diffusion coefficient of component i in the wet region. The effective gas diffusion coefficient can be expressed as follows assuming the gas phase partial pressures are small compared to the total pressure [33]:

$$D_i^{(1)} = \phi_a^{4/3} \left(\frac{\phi_a}{\phi_t}\right)^2 D_{g,i}^0 \quad (8)$$

where ϕ_a and ϕ_t are the air-filled and total porosities, respectively, and $D_{g,i}^0$ is the binary diffusion coefficient of i in air given by Fuller *et al.* [34]. The air-filled porosity is defined as $\phi_a = (1 - S_l)\phi_t$. The effective diffusion coefficient in the wet region has been investigated by Schwarzbach [35] for gas and liquid phase diffusion of a binary mixture in porous media. Assuming local equilibrium and parallel diffusion in the gas and liquid phases, an effective diffusion coefficient for the wet region can be written as follows:

$$D_i^{(2)} = D_{l,i}^{(2)} + \alpha_i D_{g,i}^{(2)} \quad (9)$$

where $D_{g,i}^{(2)}$ is the effective gas phase diffusion coefficient in the wet region given by equation (8) and $D_{l,i}^{(2)}$ is the effective liquid diffusion coefficient defined as follows:

$$D_{l,i}^{(2)} = \frac{S_l \phi_t D_{l,i}^0}{\tau}. \quad (10)$$

$D_{l,i}^0$ is the concentrated binary liquid diffusion coefficient given by Cullinen [36] and τ is the tortuosity. The concentrated binary liquid diffusion coefficient, $D_{l,i}^0$, is based on the dilute binary liquid diffusion coefficients given by Wilke and Chang [37].

The value of the liquid phase tortuosity term, τ, in equation (10) is uncertain. As the liquid saturation decreases, the tortuosity increases due to the decreased area available for liquid phase diffusion. Regions of disconnected liquid ganglia might also exist due to the low liquid saturations. The tortuosity is consequently expected to be large for the residual liquid saturations examined in this study. Thus, for modeling purposes the effective liquid diffusivity defined in equation (10) is assumed to be negligible compared to the effective vapor phase diffusivity in the wet region.

Since convective transport in the porous half-space is neglected, conservation of mass yields the following diffusion equations for the dry and wet regions, respectively:

$$\frac{\partial^2 C_i^{(1)}}{\partial z^2} - \frac{1}{\mathscr{D}_i^{(1)}} \frac{\partial C_i^{(1)}}{\partial t} = 0 \quad (11)$$

$$\frac{\partial^2 C_{l,i}^{(2)}}{\partial z^2} - \frac{1}{\mathscr{D}_i^{(2)}} \frac{\partial C_{l,i}^{(2)}}{\partial t} = 0 \quad (12)$$

where $\mathscr{D}_i^{(1)} = D_i^{(1)}/\phi_t$ and $\mathscr{D}_i^{(2)} = D_i^{(2)}/(S_l \phi_t)$. The method of Neumann [38] is used to derive an exact solution for the problem posed here. Equations (11) and (12) must be satisfied subject to the boundary conditions given in equations (3)–(6) and the initial condition given in equation (1). In the dry region the solutions to equation (11) which satisfy equation (3) for both components can be written as

$$C_i^{(1)}(z, t) = \kappa_{1,i} \operatorname{erf}\left(\frac{z}{2\sqrt{\mathscr{D}_i^{(1)} t}}\right) \quad (13)$$

where $\kappa_{1,i}$ is a constant for component i. Since the mole fractions sum to one in the liquid mixture, equation (2) can be used to yield a relation between the liquid concentrations of the two components:

$$\frac{C_{l,A}^{(2)}(z, t)}{M_A c_t} + \frac{C_{l,B}^{(2)}(z, t)}{M_B c_t} = 1. \quad (14)$$

The higher-volatility component will diffuse more quickly in the wet region according to equation (9). Therefore, the diffusion equation for the wet region [equation (12)] is applied to the more volatile component since its diffusion rate is limiting. Equation (14) is then used to express the liquid concentration of the lower-volatility component. If component A is more volatile than component B (i.e. $p_A^0 > p_B^0$) then the solution to equation (12) which satisfies boundary condition (4) and the initial condition (1) is given by

$$C_{l,A}^{(2)}(z,t) = C_{l,A}^{0} - \kappa_2 \operatorname{erfc}\left(\frac{z}{2\sqrt{\mathscr{D}_A^{(2)} t}}\right) \tag{15}$$

where κ_2 is a constant. Equations (13) and (15) can be substituted into equation (5) to determine the constants $\kappa_{1,i}$ and κ_2:

$$\kappa_{1,i} = \frac{C_{\text{sat},i}}{\operatorname{erf}\left(\dfrac{\delta(t)}{2\sqrt{\mathscr{D}_i^{(1)} t}}\right)} \tag{16}$$

$$\kappa_2 = \frac{C_{l,A}^{0} - \dfrac{C_{\text{sat,A}}}{\alpha_A}}{\operatorname{erfc}\left(\dfrac{\delta(t)}{2\sqrt{\mathscr{D}_A^{(2)} t}}\right)}. \tag{17}$$

Note that, since equations (16) and (17) must hold for all values of time, $\delta(t)$ must be proportional to $t^{1/2}$. Also, since it is assumed that the location of the evaporation front is the same for both components, $\delta(t)$ can be expressed as

$$\delta(t) = 2\lambda_A \sqrt{\mathscr{D}_A^{(1)} t} = 2\lambda_B \sqrt{\mathscr{D}_B^{(1)} t} \tag{18}$$

where λ_A and λ_B are constants. The velocity of the evaporation front is therefore proportional to $t^{-1/2}$ and is found by taking the derivative of equation (18) with respect to time.

Mass continuity at the moving evaporation front [equation (6)] is then used to determine λ_A. Substituting the expressions for the concentrations in the dry and wet regions [equations (13) and (15)–(17)] and the expression for the location of the evaporation front [equation (18)] into equation (6) yields the following continuity equations at the moving evaporation front for components A and B, respectively:

$$f_1(\lambda_A) - f_2(\lambda_A)\left(\frac{C_{l,A}^{0}}{C_{\text{sat,A}}} - \frac{1}{\alpha_A}\right) = f_3(\lambda_A) \tag{19}$$

$$f_6(\lambda_A)\frac{C_{\text{sat,B}}}{\alpha_B} + f_4(\lambda_A) = f_5(\lambda_A)\frac{C_{\text{sat,B}}}{\alpha_B} \tag{20}$$

where

$$f_1(\lambda_A) = \frac{e^{-\lambda_A^2}}{\operatorname{erf}(\lambda_A)}$$

$$f_2(\lambda_A) = \frac{D_A^{(2)}}{D_A^{(1)}}\left(\frac{\mathscr{D}_A^{(1)}}{\mathscr{D}_A^{(2)}}\right)^{1/2} \frac{e^{-\lambda_A^2 \mathscr{D}_A^{(1)}/\mathscr{D}_A^{(2)}}}{\operatorname{erfc}\left(\lambda_A\left(\dfrac{\mathscr{D}_A^{(1)}}{\mathscr{D}_A^{(2)}}\right)^{1/2}\right)}$$

$$f_3(\lambda_A) = \frac{\sqrt{\pi}\,\lambda_A S_l}{\alpha_A}$$

$$f_4(\lambda_A) = \frac{D_B^{(2)}}{\sqrt{\mathscr{D}_A^{(2)}}}\frac{M_B}{M_A} e^{-\lambda_A^2 \mathscr{D}_A^{(1)}/\mathscr{D}_A^{(2)}} \times \frac{C_{l,A}^{0}\left(1 - \dfrac{f_2(\lambda_A)}{\alpha_A(f_1(\lambda_A) - f_3(\lambda_A)) + f_2(\lambda_A)}\right)}{\operatorname{erfc}\left(\lambda_A\left(\dfrac{\mathscr{D}_A^{(1)}}{\mathscr{D}_A^{(2)}}\right)^{1/2}\right)}$$

$$f_5(\lambda_A) = \lambda_A S_l \phi_t \sqrt{\pi \mathscr{D}_A^{(1)}}$$

$$f_6(\lambda_A) = \alpha_B \frac{D_B^{(1)}}{\sqrt{\mathscr{D}_B^{(1)}}} \frac{e^{-\lambda_A^2 \mathscr{D}_A^{(1)}/\mathscr{D}_B^{(2)}}}{\operatorname{erf}\left(\lambda_A\left(\dfrac{\mathscr{D}_A^{(1)}}{\mathscr{D}_B^{(2)}}\right)^{1/2}\right)}.$$

Equations (19) and (20) represent two equations for three unknowns: λ_A, $C_{\text{sat,A}}$, and $C_{\text{sat,B}}$. Therefore one final relation must be added to close the problem. Since the liquid mole fractions must sum to one according to equation (14), an expression relating $C_{\text{sat,A}}$ and $C_{\text{sat,B}}$ can be written assuming local equilibrium exists between the gas and liquid concentrations at the evaporation front [$z = \delta(t)$]:

$$\frac{C_{\text{sat,A}}}{\alpha_A M_A C_t} + \frac{C_{\text{sat,B}}}{\alpha_B M_B c_t} = 1. \tag{21}$$

Equations (19) and (20) can be arranged to yield explicit expressions for $C_{\text{sat,A}}$ and $C_{\text{sat,B}}$ which are then inserted into equation (21) to yield the following equation as a function only of λ_A:

$$\frac{C_{l,A}^{0}}{M_A}\frac{f_2(\lambda_A)}{\alpha_A(f_1(\lambda_A) - f_3(\lambda_A)) + f_2(\lambda_A)} + \frac{1}{M_B}\frac{f_4(\lambda_A)}{f_5(\lambda_A) - f_6(\lambda_A)} - c_t = 0. \tag{22}$$

Once λ_A is obtained from equation (22), the location of the evaporation front, $\delta(t)$, is given by equation (18). Concentrations in the dry and wet regions are then determined from equations (13)–(17), which are rewritten as follows:

$$C_i^{(1)}(z,t) = \frac{C_{\text{sat},i}}{\operatorname{erf}(\lambda_i)} \operatorname{erf}\left(\frac{z}{2\sqrt{\mathscr{D}_i^{(1)} t}}\right) \tag{23}$$

$$C_{l,A}^{(2)}(z,t) = C_{l,A}^{0} - \frac{C_{l,A}^{0} - \dfrac{C_{\text{sat,A}}}{\alpha_A}}{\operatorname{erfc}\left(\lambda_A\left(\dfrac{\mathscr{D}_A^{(1)}}{\mathscr{D}_A^{(2)}}\right)^{1/2}\right)} \operatorname{erfc}\left(\frac{z}{2\sqrt{\mathscr{D}_A^{(2)} t}}\right) \tag{24}$$

$$C_{l,B}^{(2)}(z,t) = M_B\left(c_t - \frac{C_{l,A}^{(2)}(z,t)}{M_A}\right). \tag{25}$$

Finally, the average concentration of component i in the effluent gas, $C_{\text{ave},i}(t)$, can be determined by balancing the mass transfer across the surface of the porous medium at $z = 0$ with the mass carried from the system in the flowing air:

$$Q\, C_{\text{ave},i}(t) = D_i^{(1)} A_c \left.\frac{\partial C_i^{(1)}(z,t)}{\partial z}\right|_{z=0} \tag{26}$$

where Q is the air flow rate and A_c is the cross-sectional area of the porous material. By differentiating equation (23) with respect to z, evaluating the derivative at $z = 0$, and substituting the resulting relation into equation (26), the following expression for the effluent concentrations is obtained:

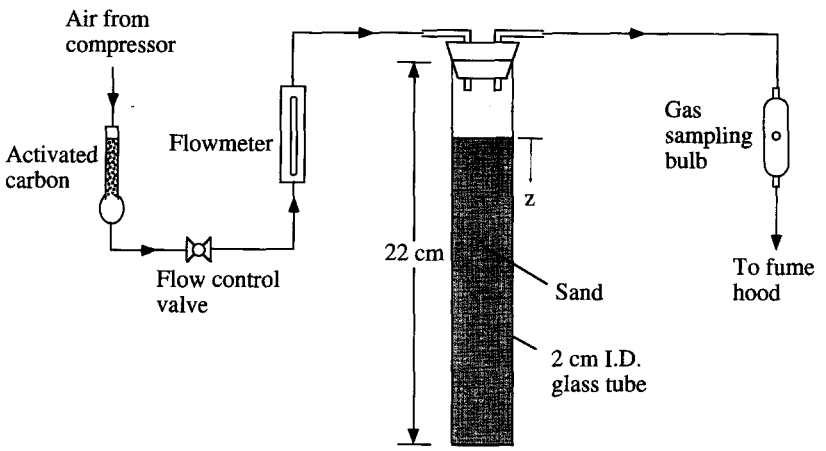

Fig. 3. Experimental apparatus for one-dimensional, external convective drying of sand.

$$C_{\text{ave},i}(t) = \frac{A_c}{Q} \frac{D_i^{(1)}}{\sqrt{\pi \mathscr{D}_i^{(1)}}} \frac{C_{\text{sat},i}}{\text{erf}(\lambda_i)} t^{-1/2}. \quad (27)$$

EXPERIMENTAL WORK

The apparatus which was used to perform the experiments is shown in Fig. 3. A compressor blows ambient air through a filter containing activated carbon which removes any hydrocarbons present in the air. The air then travels through a flowmeter before reaching a vertically oriented glass tube (2 cm diameter × 20 cm high). The tube contains 15 cm of air-dried, machine-sifted, 48–65 mesh Monterey sand (average particle diameter = 0.25 mm) with a void space at the top. The air flows into the top portion of the tube through a rubber stopper and exits through the top as well. A gas sampling bulb is located downstream of the tube so gas samples of the air stream can be taken just before the gas is exhausted into a fume hood. The porosity of the sand was determined using the mass of the sand in the tube, the density of the sand, and the total volume the sand occupied. The relative humidity of the ambient air in these experiments was between 50 and 70%.

Different binary mixtures of hydrocarbons were emplaced at variable rates (1–2 $cm^3\ min^{-1}$) into the sand from the top end of the tube with a pipette. The tube was then sealed, and the liquid was allowed to spread until the size of the wet region was observed to stabilize (3–4 days). Although the actual liquid saturation distribution may have exhibited axial variation, only the average liquid saturation was recorded based on the volume of the visibly wet region ($S_l \sim 0.1$). The airflow was initiated, and gas samples were taken frequently and analyzed through gas chromatography. The position of the evaporation front could also be observed and was recorded regularly. Then, in order to determine liquid concentrations in the remaining hydrocarbon mixture, the tube was first immersed in an ice bath. Then, the dry sand was canted off the top, and samples of wet sand were collected in separate vials at varying depths from the wet region. The gas head-space in the sealed vials was assumed to reach equilibrium with the liquid contaminant after 1–2 h. Liquid concentrations and liquid mole fractions of each sample could then be determined using head-space analysis with the gas chromatograph.

The experimental uncertainty in determining gas and liquid phase concentrations with the gas chromatograph was estimated to be within 10–20% of actual values due to calibration errors, incidental losses from the syringe or vial, and sampling variations. Other intrinsic errors resulting from experimental measurement include an estimated 10% uncertainty in both the flow rate and average liquid saturation, and a 5% uncertainty in the following parameters: porosity, volume of contaminant emplaced, and position of the evaporation front.

The experimental runs are summarized in Table 1. The same binary liquid mixture of toluene and *o*-xylene was used in runs 1–3. Different drying times were used in these three runs to investigate the changes in the liquid concentration distribution in the wet region. Also, the temperature was recorded in run 1 near the surface of the sand at $z = 0.2$ cm with a T-type thermocouple which was accurate to within $\pm 1°C$. A binary mixture of benzene and *o*-xylene was used in run 4 to determine the effects of drying a mixture of compounds of very different volatility. Finally, a mixture of toluene and octane was used in run 5 to investigate the drying behavior of a relatively non-ideal binary mixture. The vapor pressures for each of the components at 22°C are shown in Table 2 along with each component's gaseous binary diffusion coefficient in air.

RESULTS AND DISCUSSION

Figure 4 shows the experimental and predicted results for run 1. Figure 4(a) and (b) show the concentrations of each component in the effluent gas and the position of the evaporation front with time. Both the effluent concentrations and the velocity of the

Table 1. Summary of experimental runs

Experimental run	1 Toluene (A) and *o*-xylene (B)	2 Toluene (A) and *o*-xylene (B)	3 Toluene (A) and *o*-xylene (B)	4 Benzene (A) and *o*-xylene (B)	5 Toluene (A) and octane (B)
A [cm^3]	1.0	1.0	0.8	1.0	1.0
B [cm^3]	1.0	1.0	0.8	1.0	1.0
S_l	0.11	0.11	0.11	0.13	0.11
ϕ_t	0.39	0.40	0.38	0.39	0.39
T_{amb} [°C]	21	24	23	21	22
A_c [m^2]	3.4×10^{-4}	3.8×10^{-4}	3.2×10^{-4}	3.2×10^{-4}	3.4×10^{-4}
Q [m^3 s^{-1}]	1×10^{-5}	1×10^{-5}	1×10^{-5}	1×10^{-5}	1×10^{-5}
Duration, t_f [min]	8820	580	110	930	590
$\delta(t_f)$ [cm]	4.5	1.1	0.35	0.85	1.8

Table 2. Vapor pressures at 22°C [39] and binary gas diffusivities in air [34]

	p^0 [Pa]	D_g^0 [m^2 s^{-1}]
Benzene	11 000	8.8×10^{-6}
Toluene	3230	7.9×10^{-6}
Octane	1570	6.4×10^{-6}
o-Xylene	740	7.2×10^{-6}

evaporation front are seen to be proportional to $t^{-1/2}$ as predicted by the model. Figure 4(d) shows the recorded temperatures at $z = 0.2$ cm with time. The data in Fig. 4(b) reveal that the evaporation front reached $z = 0.2$ cm at 20 min, but the temperature at this location and time remained constant at the ambient temperature. Thus, the assumption of isothermal conditions in these diffusion-limited drying experiments appears to be valid. Figure 4(c) shows the experimental and predicted mass ratios of toluene to *o*-xylene in the effluent gas. The initial mass ratio in the

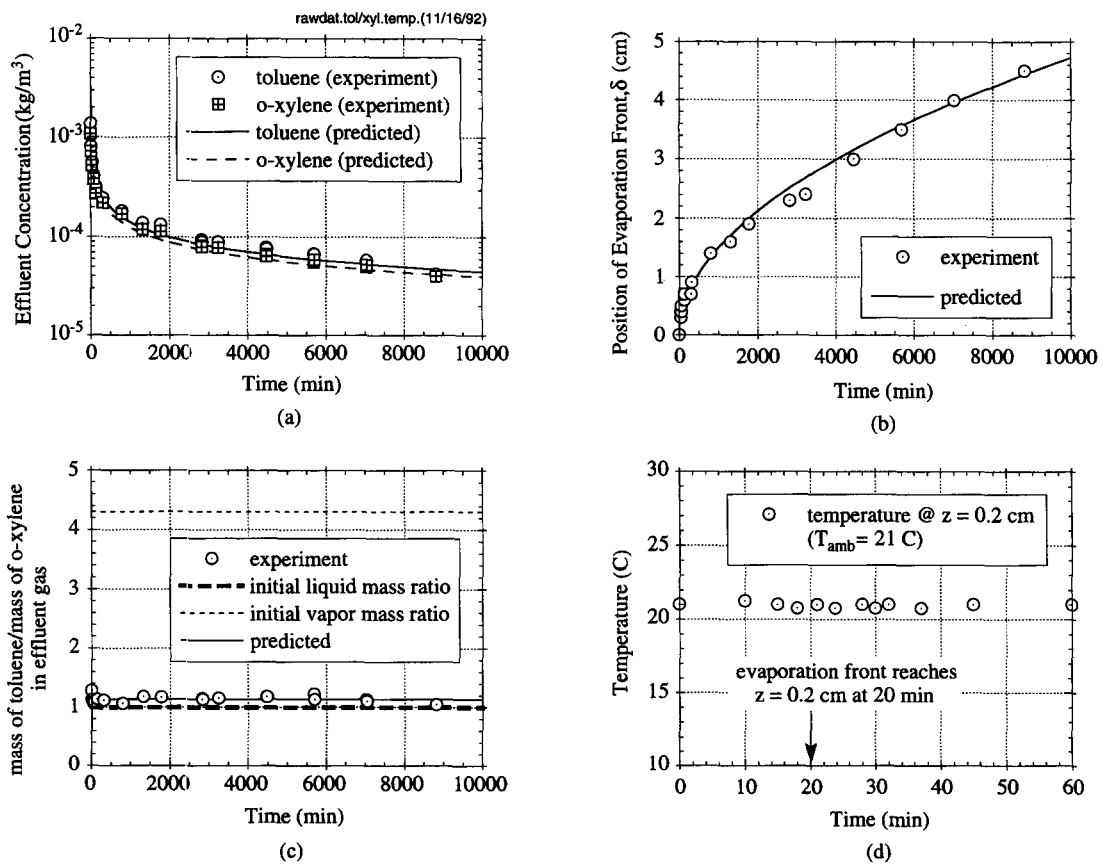

Fig. 4. Experimental and predicted values of: (a) effluent concentrations, (b) position of the evaporation front, (c) mass ratio in the effluent gas, and (d) temperatures at $z = 0.2$ cm for run 1 (1 cm^3 toluene and 1 cm^3 *o*-xylene).

liquid mixture and the initial mass ratio in the vapor phase are also shown. The measured mass ratios in the effluent gas are seen to be very close to the initial mass ratio of the liquid mixture. This contrasts with the results of selective evaporation processes such as through-flow drying in which mass ratios in the effluent gas are near the initial equilibrium mass ratio in the vapor phase.

The non-selective evaporation exhibited in these diffusion-limited cases can be explained by the existence of a variable liquid concentration zone in the wet region. Figure 5(a)–(c) shows the experimental and predicted liquid mole fraction distributions in the wet region for a mixture of toluene and *o*-xylene at different times. A single evaporation front of both compounds propagates into the contaminated region, confirming the assumption of a single evaporation front in the theoretical model. As the evaporation front penetrates into the sand, a zone of variable liquid mole fractions is seen to grow in length ahead of the front due to continual evaporation and diffusion from within the wet region. Due to the higher volatility of toluene, its liquid mole fraction is lower than that of *o*-xylene at the evaporation front. However, a large resistance to mass transfer in the wet region causes the liquid mole fractions farther away from the evaporation front (as $z \to \infty$) to remain at the initial mole fractions, x_A^0 and x_B^0, of the emplaced liquid. This non-uniform distribution of the liquid mole fractions of the high and low volatility compounds in the wet region yields the constant observed mass fractions in the effluent gas shown in Fig. 4(c). Note that the experiment and theory disagree at long times in Fig. 5(c). The discrepancy is postulated to result from the finite length of the contaminated region in the experiment. The theoretical assumption of an infinite domain becomes invalid when the zone of variable liquid concentrations extends to the boundary of the contaminated region. This occurs sometime between 580 and 8820 min as shown in Fig. 5(b) and (c).

Similar behavior was observed during the evaporation of a binary mixture of benzene and *o*-xylene (run 4). The results are shown in Fig. 6. The purpose of this run was to determine if the evaporation would remain non-selective even though the volatility of benzene is much greater than that of *o*-xylene. Figure 6(a) and (b) shows the effluent concentrations and evaporation front position, $\delta(t)$, with time. The model overpredicts $\delta(t)$ and underpredicts the effluent concentrations, but the trends in the data are represented by the predicted behavior. Slight variations in the liquid saturation, S_l, strongly affect the calculated values of both $\delta(t)$ and the effluent concentrations. Therefore, since an average liquid saturation was used in the model for the entire visibly wet region, discrepancies may be caused by a non-uniform distribution of the emplaced liquid. Figure 6(c) shows the experimental and predicted mass ratios of benzene to *o*-xylene in the effluent gas. Again, the evaporation is seen to be non-selective even in the case of very

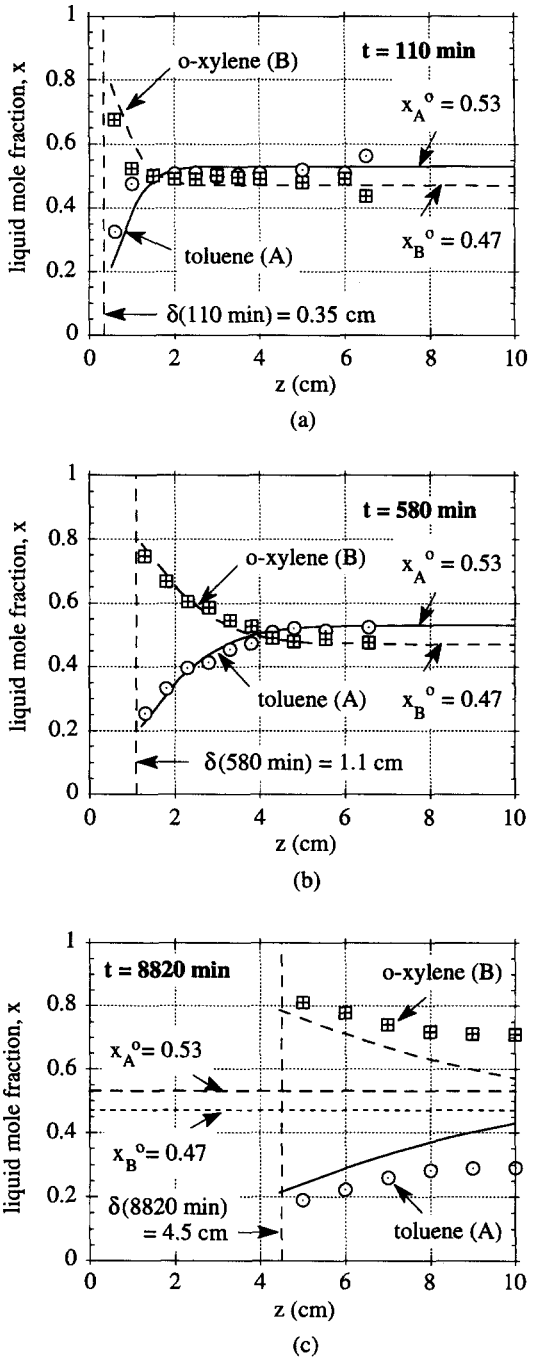

Fig. 5. Experimental and predicted liquid mole fraction distribution of toluene and *o*-xylene in the wet region at: (a) 110 min, (b) 580 min, and (c) 8820 min.

different volatility compounds. The vapor pressure ratio of benzene to *o*-xylene is 15 : 1, but the measured mass ratio in the effluent gas is only about 1.5 : 1, which is relatively close to the initial mass ratio, 1 : 1, of the emplaced liquid mixture. Figure 6(d) shows the liquid mole fractions of benzene and *o*-xylene in the wet region at 930 min. Again, a zone of variable liquid mole fractions is seen to exist in the wet region ahead of the evaporation front. The predicted liquid mole

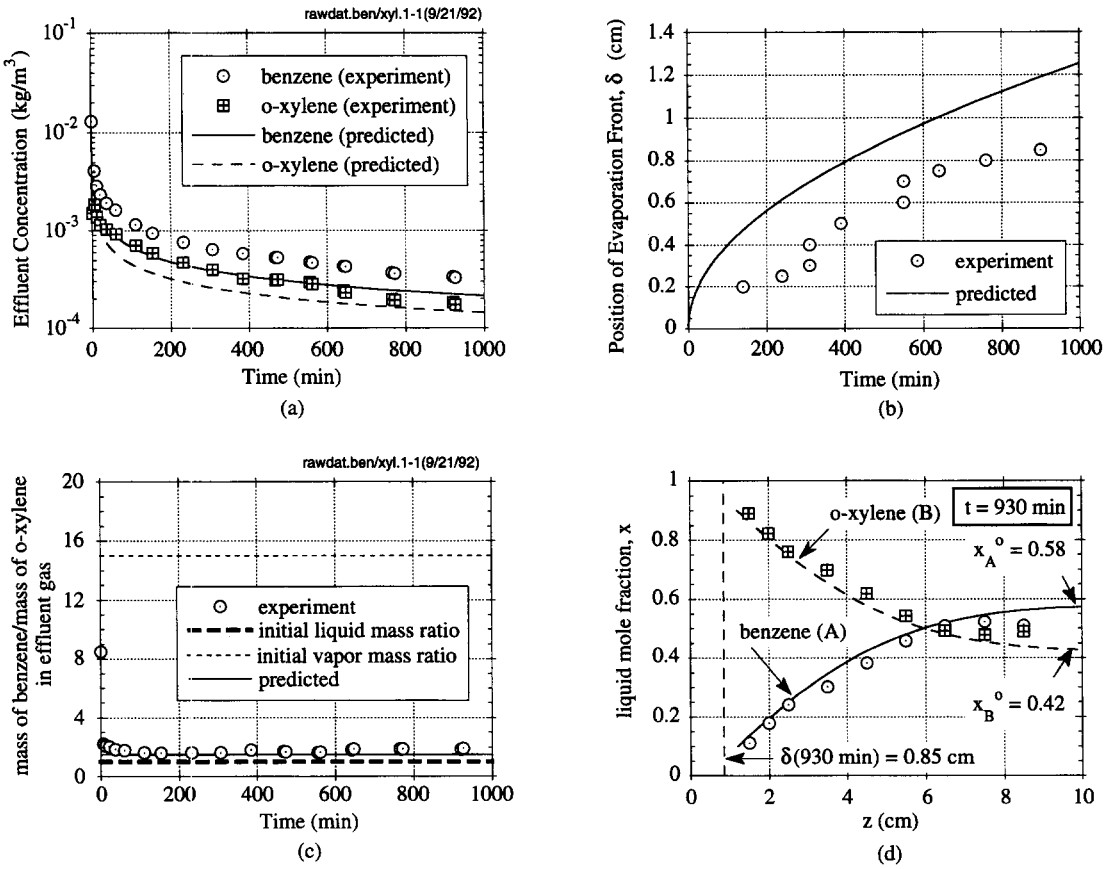

Fig. 6. Experimental and predicted values of: (a) effluent concentrations, (b) position of the evaporation front, (c) mass ratio in the effluent gas, and (d) liquid mole fractions for run 4 (1 cm^3 benzene and 1 cm^3 *o*-xylene).

fraction distribution is seen to agree well with the experimental data.

A relatively non-ideal mixture of toluene and octane was used in run 5. Although the activity coefficients of these compounds deviate slightly from one [40], an ideal mixture was assumed in the model ($\gamma_{il} = 1$) to see how the predicted results would compare to the experimental data for this non-ideal mixture. Figure 7(a) and (b) shows the effluent concentrations and position of the evaporation front with time. The model results are seen to be in close agreement with the data. Figure 7(c) shows the mass ratios of toluene to octane in the effluent gas, and the data again reveal a non-selective evaporation process. Figure 7(d) shows the liquid mole fraction distribution in the wet region at 590 min. Since the compounds are fairly similar in volatility, there is not as much segregation between the mole fractions at the evaporation front as there was for benzene and *o*-xylene in run 4. As with the other mixtures, the trend of the data matches well with the predicted distribution of liquid mole fractions.

Recall that the liquid phase diffusivity was assumed to be negligible compared to the gas phase diffusivity for the runs in this study. Since the predicted results were shown to be in good agreement with the experimental data, the dominant mode of transport in the wet region for the compounds used in this study appears to be gas phase diffusion. Under this assumption, the effective diffusivity in the wet region can be quite different for each compound of a liquid mixture, depending on the vapor pressure of the compound. The most volatile component will have the largest effective diffusivity and will have a dominant influence on the length of the zone of variable liquid concentrations in the wet region.

In all of the previous runs, non-selective evaporation was observed and the mass ratio of the compounds in the effluent concentration were seen to reach a constant value in a relatively short time. Heimann *et al.* [32] discuss the time required to reach this steady value during the constant rate period of drying assuming a constant liquid velocity due to capillary suction. They conclude that for a mixture of isopropyl alcohol and water the steady-state liquid concentration profile is reached within several minutes. Similar drying times to reach a constant effluent mass ratio were found in this study. In addition, these drying times were seen to depend on the volatility of the components. If the mixture contained a low-volatility component, then the time required to reach a constant mass ratio in the effluent gas was longer. To understand this behavior, consider the initial moments when

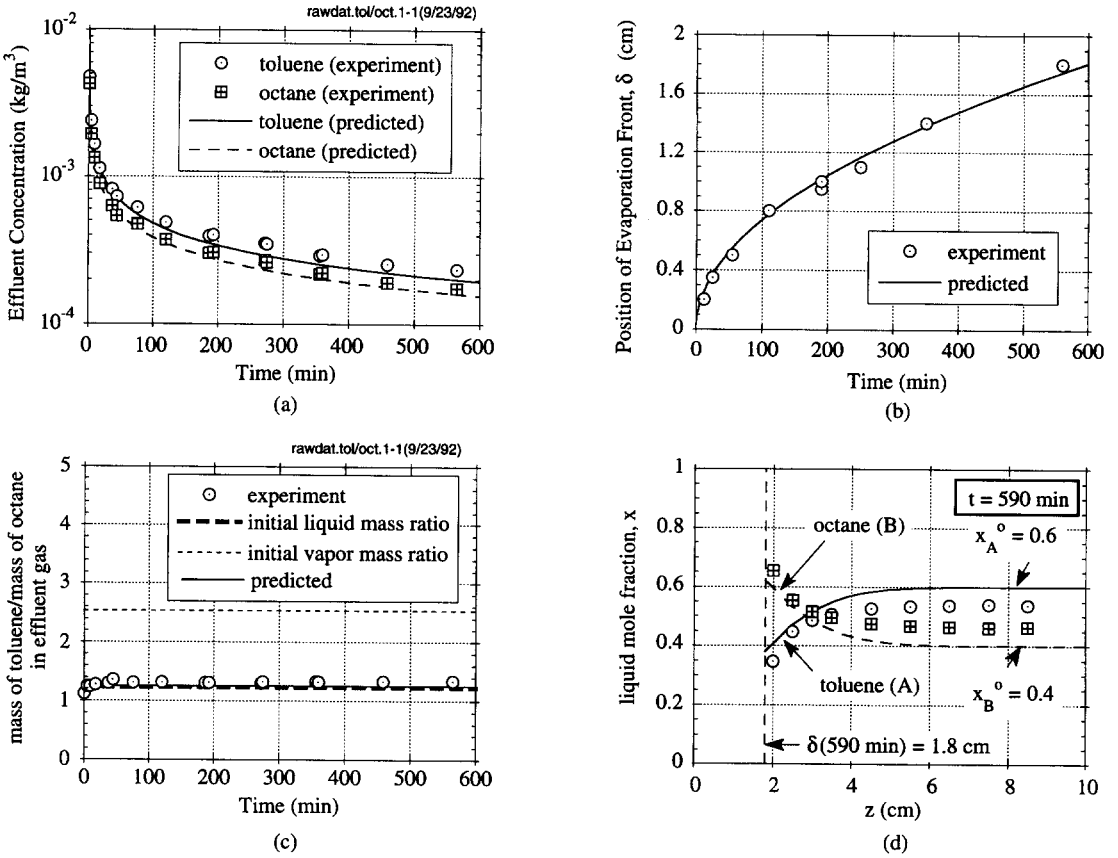

Fig. 7. Experimental and predicted values of: (a) effluent concentrations, (b) position of the evaporation front, (c) mass ratio in the effluent gas, and (d) liquid mole fractions for run 5 (1 cm³ toluene and 1 cm³ octane).

the wet region is exposed to the external flow; the conditions are identical to through-flow drying and selective evaporation is expected. Therefore, the time required to reach a steady mass ratio in the effluent gas should correlate with the time required for the evaporation front to penetrate a certain distance into the porous material such that a dry region exists between the liquid and the convective flow. At that time, transport is due only to diffusion, and a constant mole fraction ratio at the evaporation front is established to satisfy mass conservation between the wet and dry regions.

This study considered a semi-infinite region, but, if the porous material is finite in the z-direction, the evaporation is postulated to exhibit three stages based on the results of this study:

(1) Initially, a selective evaporation occurs in which the more volatile component is removed preferentially from the exposed liquid surface at $z = 0$. The liquid mole fraction of the higher-volatility component decreases at the evaporating surface which corresponds to a decrease in the mass fraction of the higher-volatility component in the effluent gas.

(2) As the evaporation front penetrates into the porous material, a non-selective evaporation is characterized by constant component mass fractions in the effluent gas which are near the initial component mass fractions in the emplaced liquid mixture.

(3) As the evaporation front propagates toward the bottom of the porous material, the length of the zone of variable liquid concentrations will eventually exceed the length of the porous material. The mass fraction of the higher-volatility component in the effluent gas will then gradually decrease to zero due to the depleted liquid mole fractions of the higher-volatility component throughout the remaining wet region.

These three stages were observed by Ho and Udell [16] during two-dimensional drying experiments with toluene and *o*-xylene.

Finally, since the mass ratio of the compounds in the effluent gas reaches a steady value near the mass ratio of the initial liquid, a simplified analysis can be performed to determine the effluent gas concentrations. Assuming that the mass ratio of the effluent concentrations is equal to the mass ratio of the emplaced liquid, Ho and Udell [16] showed that the liquid mole fractions at the penetrating evaporation front can be determined for a binary mixture. In fact, liquid mole fractions for mixtures with multiple components can be determined using the same method. Then, if local equilibrium exists and a linear gas phase

concentration distribution in the dry region is assumed, the effluent concentrations for each component can be determined by a simple mass balance given in equation (26). The assumption of a linear gas phase concentration distribution in the dry region appears to be valid since the equation derived in this report for the gas phase concentrations [equation (23)] exhibits a nearly linear distribution.

CONCLUSIONS

A one-dimensional analytic model was developed for external convective drying of porous materials containing an immobile binary liquid mixture. The model predicts effluent gas concentrations, liquid concentrations, and positions of the evaporation front assuming isothermal and uniformly saturated conditions. One-dimensional experiments were performed with several binary hydrocarbon mixtures to verify the validity of the model. Based on the findings of this study, the following conclusions can be made:

(1) Diffusion-limited evaporation is non-selective in terms of removing the higher volatility component during external convective drying of porous media containing immobile binary liquid mixtures. Mass fractions in the effluent gas remain near the initial mass fractions of the liquid mixture.

(2) A growing zone of variable liquid concentrations exists within the wet region near the penetrating evaporation front. The length of this variable-concentration zone is determined by the gas phase diffusivity of the more volatile component.

(3) Both the velocity of the evaporation front and the effluent concentrations are proportional to $t^{-1/2}$ and are strongly dependent on liquid saturation. At higher liquid saturations, the velocity of the evaporation front decreases, and the effluent concentrations increase.

Acknowledgements—This study was performed with financial support from NIEHS Grant No. 3 P42ES04705-0251 and EPA Award No. R-815247-01-0.

REFERENCES

1. N. H. Ceaglske and O. A. Hougen, Drying granular solids, *Ind. Engng Chem.* **29**(7), 805–813 (1937).
2. A. V. Luikov, *Heat and Mass Transfer in Capillary-porous Bodies*. Pergamon Press, Oxford (1966).
3. A. V. Luikov, Systems of differential equations of heat and mass transfer in capillary-porous bodies (review), *Int. J. Heat Mass Transfer* **18,** 1–14 (1975).
4. S. Whitaker, Heat and mass transfer in granular porous media. In *Advances in Drying* (Edited by A. S. Mujumdar), Vol. 1, pp. 23–61. Hemisphere, Washington, DC (1980).
5. M. Fortes and M. R. Okos, Drying theories: their bases and limitations as applied to foods and grains. In *Advances in Drying* (Edited by A. S. Mujumdar), Vol. 1, pp. 119–154. Hemisphere, Washington, DC (1980).
6. J. Van Brakel, Mass transfer in convective drying. In *Advances in Drying* (Edited by A. S. Mujumdar), Vol. 1, pp. 217–267. Hemisphere, Washington, DC (1980).
7. R. Toei, Drying mechanism of capillary porous bodies. In *Advances in Drying* (Edited by A. S. Mujumdar), Vol. 2, pp. 269–297. Hemisphere, Washington, DC (1983).
8. N. Schadler and W. Kast, Experimental studies and mathematical modelling on convective drying of porous bodies. In *Drying of Solids: Recent International Developments* (Edited by A. S. Mujumdar), pp. 29–40. John Wiley, New York (1986).
9. S. Szentgyörgyi, Some theoretical aspects of drying of solids. In *Advances in Drying* (Edited by A. S. Mujumdar), Vol. 4, pp. 147–198. Hemisphere, Washington, DC (1987).
10. J. G. Hartley, Coupled heat and moisture transfer in soils: a review. In *Advances in Drying* (Edited by A. S. Mujumdar), Vol. 4, pp. 199–248. Hemisphere, Washington, DC (1987).
11. S. B. Nasrallah and P. Perre, Detailed study of a model of heat and mass transfer during convective drying of porous media, *Int. J. Heat Mass Transfer* **31,** 957–967 (1988).
12. P. Chen and P. S. Schmidt, An integral model for convective drying of hygroscopic and nonhygroscopic materials. In *Drying* '89 (Edited by A. S. Mujumdar and M. Roques), pp. 162–168. Hemisphere, Washington, DC (1990).
13. W. Masmoudi and M. Prat, Heat and mass transfer between a porous medium and a parallel external flow. Application to drying of capillary porous materials, *Int. J. Heat Mass Transfer* **34,** 1975–1989 (1991).
14. E. U. Schlünder, Selective drying of mixture-containing products. In *Drying* '89 (Edited by A. S. Mujumdar and M. Roques), pp. 9–23. Hemisphere, Washington, DC (1990).
15. P. C. Johnson, C. C. Stanley, M. W. Kemblowski, D. L. Byers and J. D. Colthart, A practical approach to the design, operation, and monitoring of in situ soil-venting systems, *Ground Wat. Monit. Rev.* **10**(2), 159–178 (1990).
16. C. K. Ho and K. S. Udell, An experimental investigation of air venting of volatile liquid hydrocarbon mixtures from homogeneous and heterogeneous porous media, *J. Contam. Hydrol.* **11**(3), 1–26 (1992).
17. K. Rainwater, M. R. Zaman, B. J. Claborn and H. W. Parker, Experimental and modeling studies of in situ volatilization: vapor–liquid equilibrium or diffusion-controlled process?, *Proceedings of NWWA/API Conference on Petroleum Hydrocarbons and Organic Chemicals in Ground Water*, pp. 457–472 (1989).
18. K. Rathfelder, W. W.-G. Yeh and D. Mackay, Mathematical simulation of soil vapor extraction systems: model development and numerical examples, *J. Contam. Hydrol.* **8,** 263–297 (1991).
19. L. N. Gupta, An approximate solution of the generalized Stefan's problem in a porous medium, *Int. J. Heat Mass Transfer* **17,** 313–321 (1974).
20. S. H. Cho, An exact solution of the coupled phase change problem in a porous medium, *Int. J. Heat Mass Transfer* **18,** 1139–1142 (1975).
21. M. D. Mikhailov, Exact solution of temperature and moisture distributions in a porous half-space with moving evaporation front, *Int. J. Heat Mass Transfer* **18,** 797–804 (1975).
22. S. Szentgyörgyi and K. Molnár, Calculation of drying parameters for the penetrating evaporation front. In *Drying* '84 (Edited by A. S. Mujumdar), pp. 76–82. Hemisphere, Washington, DC (1984).
23. S. Szentgyörgyi, K. Molnár and M. Örvös, Computer calculation method of the falling rate period of drying. In *Drying* '84 (Edited by A. S. Mujumdar), pp. 83–87. Hemisphere, Washington, DC (1984).
24. S. Szentgyörgyi and M. Örvös, An approximation method for the determination of the distribution of temperature and of moisture content in the falling rate period of drying, *Drying Technol.* **3**(3), 399–419 (1985).
25. E. Mitura, S. Michalowski and W. Kaminski, A math-

ematical model of convection drying in the falling drying rate period, *Drying Technol.* **6**(1), 113–137 (1988).
26. A. L. Baehr, G. E. Hoag and M. C. Marley, Removing volatile contaminants from the unsaturated zone by inducing advective air-phase transport, *J. Contam. Hydrol.* **4,** 1–26 (1989)
27. M. C. Marley and G. E. Hoag, Induced soil venting for recover/restoration of gasoline hydrocarbons in the vadose zone, *Proceedings of NWWA/API Conference on Petroleum Hydrocarbons and Organic Chemicals in Ground Water*, pp. 473–503 (1984).
28. S. Lingineni and V. K. Dhir, Modeling of soil venting processes to remediate unsaturated soils, *ASCE J. Envir. Engng* **118**(1), 135–152 (1992).
29. C. K. Ho and K. S. Udell, A mass transfer model for the removal of a volatile organic compound from heterogeneous porous media during vacuum extraction, *ASME Heat Transfer Geophys. Media* **172,** 55–62 (1991).
30. F. Thurner and E. U. Schlünder, Convective drying of porous materials containing binary mixtures. In *Drying* '85 (Edited by R. Toei and A. S. Mujumdar), pp. 117–125. Hemisphere, Washington, DC (1985).
31. R. M. Cunningham and J. J. Kelly, Liquid transport in drying macroporous materials. In *Drying* '80 Vol. 1: *Developments in Drying* (Edited by A. S. Mujumdar), pp. 40–47. Hemisphere, Washington, DC (1980).
32. F. Heimann, F. Thurner and E. U. Schlünder, Intermittent drying of porous materials containing binary mixtures, *Chem. Engng Process.* **20,** 167–174 (1986).
33. R. J. Millington, Gas diffusion in porous media, *Science* **130,** 100–102 (1959).
34. E. N. Fuller, P. D. Schettler and J. C. Giddings, A comparison of methods for predicting gaseous diffusion coefficients, *J. Gas Chromat.* 222–227 (1965).
35. J. Schwarzbach, Diffusion in porous materials partially wetted with a binary mixture, *Chem. Engng Process.* **26,** 35–44 (1989).
36. H. T. Cullinan, Concentration dependence of the binary diffusion coefficient, *Ind. Engng Chem. Fundam.* **5,** 281–283 (1966).
37. C. R. Wilke and P. Chang, *A.I.Ch.E. J.* **1,** 264 (1955).
38. H. S. Carslaw and J. C. Jaeger, *Conduction of Heat in Solids*, pp. 282–286. Clarendon Press, Oxford (1959).
39. R. H. Perry and D. Green, *Perry's Chemical Engineer's Handbook*. McGraw-Hill, New York (1984).
40. E. W. Funk and J. M. Prausnitz, Thermodynamic properties of liquid mixtures: aromatic-saturated hydrocarbon systems, *Ind. Engng Chem.* **62**(9), 8–15 (1970).